ORIGINAL PAPER

Effects of alternative splicing events and transcriptome changes on kidney stone formation

Qunsheng Yan[1,2,3] · Yang Chen[1,2,3] · Haoran Liu[1,2,3] · Guoxiang Li[1,2,3] · Chaozhao Liang[1,2,3] · Zongyao Hao[1,2,3]

Abstract

During the development of urinary stone disease, the formation of tiny crystals that adhere to the renal tubular epithelium induces epithelial cell damage. This damage and repair of the epithelium is associated with the establishment of more crystal adhesion sites, which in turn stimulates further crystal adhesion and, eventually, stone formation. Deposited crystals typically cause changes in epithelial cell gene expression, such as transcriptome changes and alternative splicing events. Although considered important for regulating gene expression, alternative splicing has not been reported in studies related to kidney stones. To date, whether alternative splicing events are involved in the regulation of stone formation and whether crystallographic cell interactions are regulated by alternative splicing at the transcriptional level have remained unknown. Therefore, we conducted RNA sequencing and alternative splicing-related bioassays by modeling the in vitro stone environment. Many alternative splicing events were associated with crystallographic cell interactions. Moreover, these events regulated transcription and significantly affected the capacity of crystals to adhere to renal tubular epithelial cells and regulate apoptosis.

Keywords RNA-seq · Kidney stone · Nephrocalcinosis · Alternative splicing

Introduction

The incidence of renal stone disease has more than doubled in the past 40 years, with between 7 and 11% of the population at risk of kidney stone-related symptoms each year [1]. The formation of urinary stones involves several microscopic processes, such as crystal formation, adhesion and growth [2]. During these processes, renal tubular epithelial cells closely interact with adherent crystals, which affect cell adhesion, apoptosis, and inflammatory responses [3–5]. These interactions play important roles in the eventual formation of stones.

Alternative splicing events (ASEs) have been widely reported to be of importance for the regulation of gene expression, but related results exhibit some differences in kidney stones and kidney stone-related injury. Previously, the specific impact of selective splicing associated with damage caused by crystal deposition was unknown; however, we carried out relevant RNA sequencing (RNA-seq) analyses, focusing on splicing. We used calcium oxalate nodule nanocrystals to treat renal tubular epithelial cells, after harvesting the cells, performed high-throughput sequencing. The aim was to discover associations between differential ASEs occurring at the transcriptional level and differentially expressed genes (DEGs). The analysis revealed an alternative splicing (AS) regulation mechanism during crystal–cell interactions. We identified many ASEs and their important roles in CaOx-induced anomalous transcriptional regulation, particularly related to cell adhesion and apoptosis.

Qunsheng Yan and Yang Chen contributed equally to this work.

✉ Chaozhao Liang
liang_chaozhao@ahmu.edu.cn

✉ Zongyao Hao
haozongyao@163.com

1   Department of Urology, The First Affiliated Hospital of Anhui Medical University, Hefei, China

2   Institute of Urology, Anhui Medical University, Hefei, China

3   Anhui Province Key Laboratory of Genitourinary Diseases, Anhui Medical University, Hefei, China

Methods

Modeling and RNA sequencing

We used calcium oxalate stones previously collected in the clinic to obtain calcium oxalate stone nanocrystals by a process comprising ball milling and pulverization [6]. Calcium oxalate nanocrystals were subsequently cultured with renal tubular epithelial cells at a concentration of 100 μg/ml for 24 h (3 replicates) to establish a treatment group. Renal tubular epithelial cells grown normally for 24 h (3 replicates) were used as the control group. HK-2 cells were purchased from Nanjing Institute of Biology, Chinese Academy of Sciences, and cultured in Dulbecco's modified Eagle medium–nutrient mixture F-12 (DMEM-F12) with 10% fetal bovine serum in an incubator at 37 °C with 5% CO_2. The RNA-seq data obtained from the treatment and control groups were evaluated to identify ASEs and DEGs. Moreover, functional clustering analyses (Gene Ontology [GO] and Kyoto Encyclopedia of Genes and Genomes [KEGG]) of DEGs were performed.

Read alignment and differentially expressed gene analysis

Clean reads were aligned to Genome Reference Consortium Human Build 38 (GRch38) by TopHat2 [7], which revealed 4 mismatches. Uniquely mapped reads were ultimately used to calculate the read number and reads per kilobase of exons per million fragments mapped (RPKM) for each gene. The expression levels of DEGs were assessed based on RPKM. EdgeR software [8], specifically designed for the analysis of differential gene expression, was applied to screen the RNA-seq data for DEGs. The results were analyzed using fold change (FC) ≥ 2 or ≤ 0.5 and false discovery rate (FDR) ≤ 0.05 criteria to identify DEGs.

Validation of differentially expressed genes by RT-qPCR

The specificity of the primers was verified by Prime-Blast, which is a tool designed for identifying significantly differentially expressed RNAs. Total RNA was extracted from HK-2 cells and control cells treated with calcium oxalate stone nanocrystals. The concentration and purity of RNA were found to meet the established requirements. A Takara-series RT-qPCR kit was used for reverse transcription and quantitative amplification. The cycle threshold (CT) values were corrected by the -ΔΔ CT method.

Subsequently, relative RNA expression and significant differences in expression were calculated ($P < 0.05$).

Alternative splicing analysis

Inter-sample alternative splicing events and regulated alternative splicing events (RASEs) were identified and quantitated using the ABL pipeline, as described previously [9, 10]. In brief, the ABL pipeline enables the detection of ten types of ASEs based on splice junction reads, namely exon skipping (ES), alternative 5' splice site (A5SS), alternative 3' splice site (A3SS), intron retention (IR), mutually exclusive exon (MXE), mutually exclusive 5' untranslated region (UTR; 5pMXE), mutually exclusive 3' UTR (3pMXE), cassette exon, A3SS&ES and A5SS&ES ASEs. For sample pair comparisons, Fisher's exact test was used to determine statistical significance based on the alternative reads and model reads of the samples used as input data. We calculated the change ratio of alternatively spliced reads and constitutively spliced reads between compared samples, which was defined as the RASE ratio. A RASE ratio ≥ 0.2 and p value ≤ 0.05 were set as thresholds for RASE detection. For comparisons of repeated analyses, Student's t test was used to evaluate significant changes in the RASE ratio. Events that were found to be significant at the p value cut-off of 0.05 were considered RASEs.

Functional enrichment analysis

To sort DEGs, Gene Ontology (GO) terms and KEGG pathways into functional categories, the KEGG Ortholog-Based Annotation System (KOBAS) 2.0 server was used [11]. Hypergeometric tests and Benjamini–Hochberg-based false discovery rate (FDR) control procedures were used to determine the enrichment of each term. Reactome (http://reactome.org) pathway profiling was also performed in the functional enrichment analysis of selected gene sets.

Other statistical analyses

Principal component analysis (PCA) was performed with the R package factoextra (https://cloud.r-project.org/package=factoextra), which shows the clustering of samples with the first two components. After normalizing the reads of each gene in the samples by tags per million (TPM), an in-house script (Sogen) was used to visualize next-generation sequence data and genomic annotations. The pheat map package in R was used to perform clustering (https://cran.r-project.org/web/packages/pheatmap/index.html) based on Euclidean distances. Student's t test was used to compare two groups. We used the global test [12, 13] to determine the association of the normalized gene expression levels of

RNA-binding proteins (RBPs) in different samples with different phenotypes.

Results

Crystal stimulation leads to significant alterations in gene expression

Analysis of DEGs in calcium oxalate stone nanocrystal-treated renal tubular epithelial cells compared with control cells revealed significant alterations in gene expression.

A total of 33,205 genes were identified, of which 416 were significantly upregulated and 108 were downregulated (Fig. 1A). The results of GO and KEGG enrichment analyses revealed that most DEGs were associated with cell adhesion, inflammatory responses, inflammatory mediator (e.g., arachidonic acid) secretion and other processes (Figs. 1 and 2) as well as with human autoimmune diseases such as systemic lupus erythematosus and rheumatoid arthritis. The cell adhesion pathway, which was significantly associated with upregulated genes, was the focus of our attention. In

previous studies, cell crystal adhesion was found to play an important role in the development of kidney stones, acting as a key factor in the stone formation process. Upregulated genes were mostly involved in cellular activities such as the regulation of intracellular factor receptors, activation of RNA enzymes, and methylation of DNA (Fig. 2C). These genes might have a regulatory role at the cellular transcriptional level in promoting the deposition of kidney crystals.

Genes associated with the negative regulation of apoptosis and cell adhesion pathways were downregulated, indicating decreased expression of genes associated with apoptosis inhibition. These events might be associated with the regulation of renal tubular epithelial injury. Apoptosis, as a type of programmed death, enables the body to clear damaged or senescent cells without inducing an acute inflammatory response. Accordingly, downregulation of genes involved in local negative apoptosis regulation may amplify the inflammatory response and the deposition of crystals. Furthermore, these downregulated genes may significantly affect the expression of cell adhesion molecules (CAMs) and the processing of mitochondrial tRNAs and rRNAs (Fig. 2D). These observations are in line with previous results that
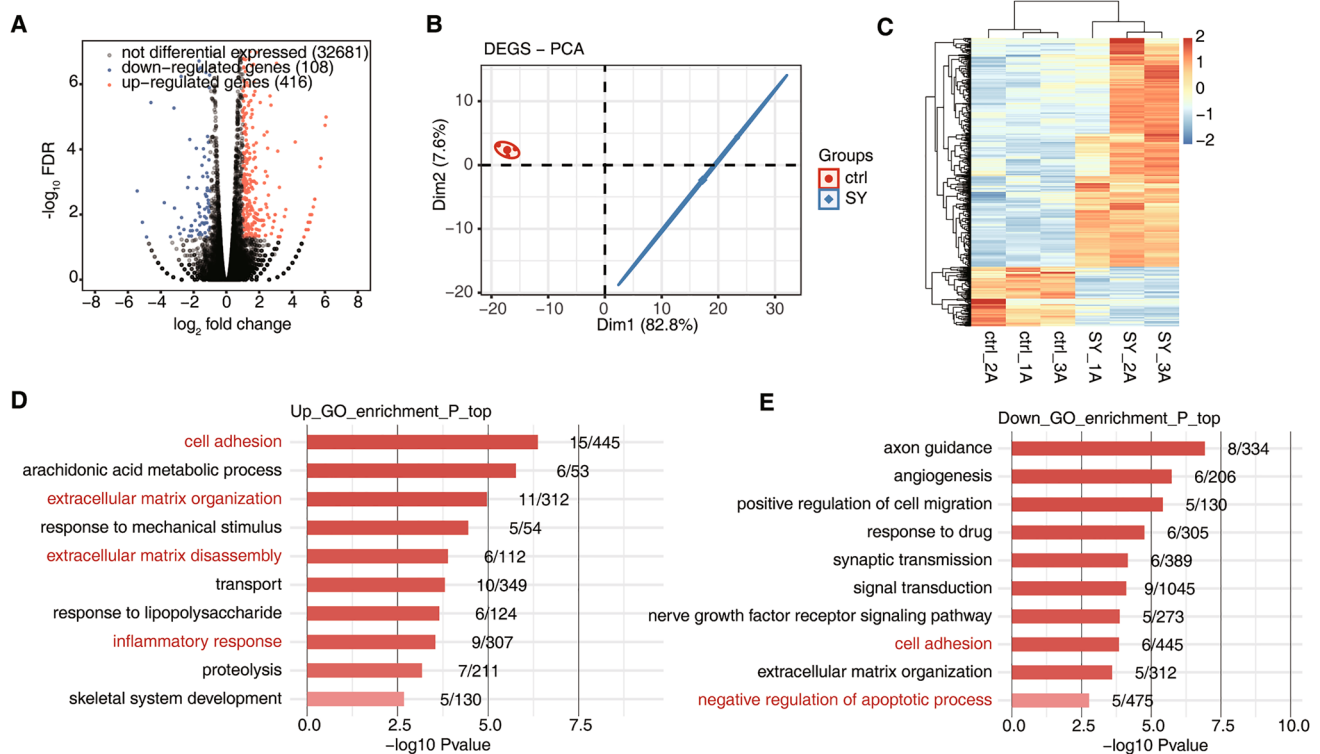
Fig. 1 Transcriptome analysis of differentially expressed genes (DEGs) between renal tubular epithelial cells in which sodium oxalate crystallization was induced and control cells. **A** Volcano plots showing DEGs between SY and Ctrl samples. A false discovery rate (FDR) ≤ 0.05 and a fold change (FC) ≥ 2 or ≤ 0.5 were the criteria for DEG identification. **B** Principal component analysis (PCA) of SY and control (Ctrl) samples in human renal tubular epithelial cells was based on the fragments per kilobase of transcript per million reads (FPKM) values of all DEGs. The ellipse of each group is the confidence ellipse. **C** Heat map of 3SY and 3Ctrl samples based on all DEG FPKM values. **D**, **E**. Gene Ontology (GO) analysis of DEGs categorized into upregulated genes (**D**) and downregulated genes (**E**)
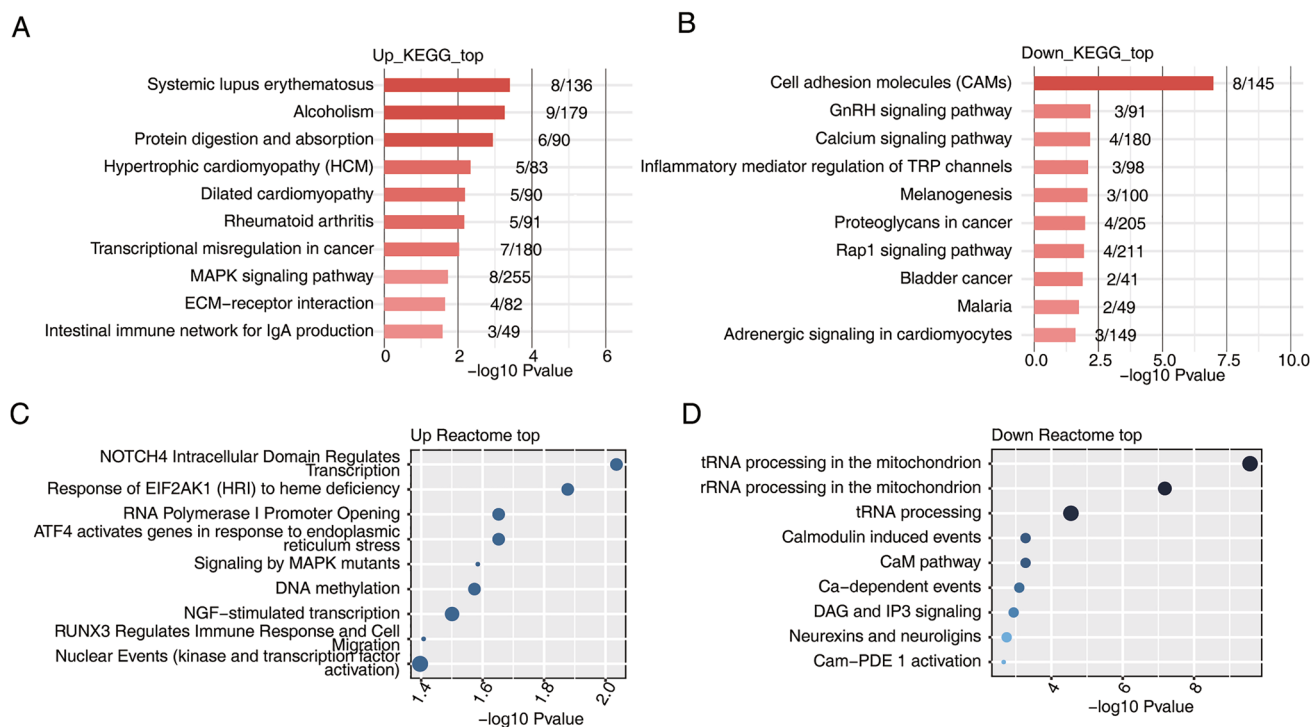
Fig. 2 Functional pathway analysis of differentially expressed genes (DEGs) in SY and Ctrl samples of human renal tubular epithelial cells. **A**, **B** Kyoto Encyclopedia of Genes and Genomes (KEGG) analysis of the DEGs categorized into up- and downregulated genes. **C**, **D** Reactome analysis of DEGs categorized into up- and downregulated genes

showed changes in cellular function during crystal deposition and oxidative damage to mitochondria.

RT-qPCR experiments revealed the accuracy and consistency of the sequencing results

For validation of the results, we randomly selected two genes that were significantly differentially expressed. Real-time fluorometric qPCR was used to amplify and obtain CT values, and the relative expression of RNA was calculated by the -$\Delta\Delta$CT value-correction method. The RT-qPCR results were found to be in general agreement with the sequencing results (Fig. 3B). The results from the experiments showed that differences in gene expression were reasonably consistent and provided a basis for further research.

Identification of many alternative splicing events

We identified many differential ASEs. These differential ASEs were analyzed to determine how effectively they distinguished the treatment group from the control group (Fig. 4B, C). Among the nine differential splicing events that we evaluated, ASEs were most frequent for A5SSs and A3SSs (Fig. 5), and among the DEGs, most ASEs involved ES (exon skipping), an A5SS (alternative 5' splice site) or an A3SS (alternative 3' splice site) (Fig. 4A). Genes that

underwent selective splicing were most commonly enriched in transcriptional regulation, mismatch repair and related pathways.

Target genes of transcription factors (TFs) that undergo differential AS were extracted from the Ensembl database and Transcriptional Regulatory Relationships Unraveled by Sentence-based Text mining (TRRUST) database. Then, the target genes that overlapped with DEGs were identified, and many of these DEGs were found to be potentially regulated by the assessed TFs (Fig. 4E, F).

TF (with RAS) targets that overlap DEGs in functional enrichment analysis

We selected a set of genes from the larger group of genes with expression affected by TFs in which variable splicing events had been identified. We analyzed this gene set, TF gene targets that had undergone RASEs and DEGs by generating a Venn diagram. We found many intersecting genes, suggesting that these variable splicing events influenced the differential expression of related genes (Fig. 4F). GO and KEGG analyses revealed that these overlapping genes regulated by variable splicing events were highly enriched in cell adhesion, cellular response, inflammatory response, cell migration and other pathways associated with renal calculi.
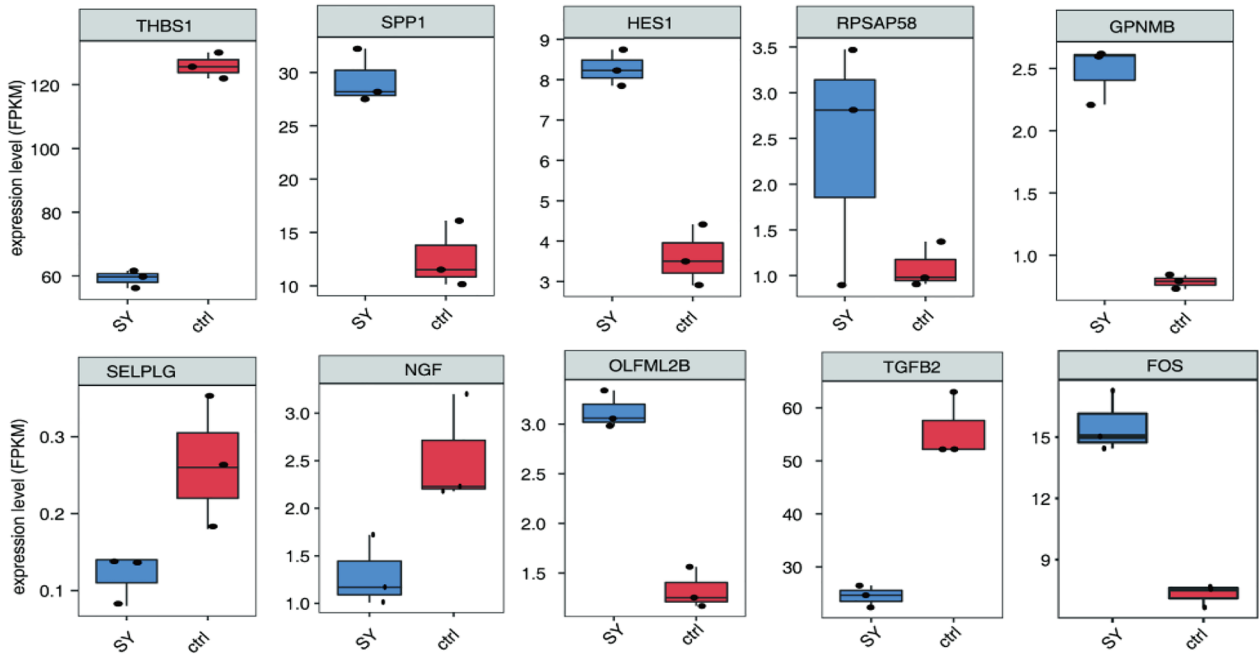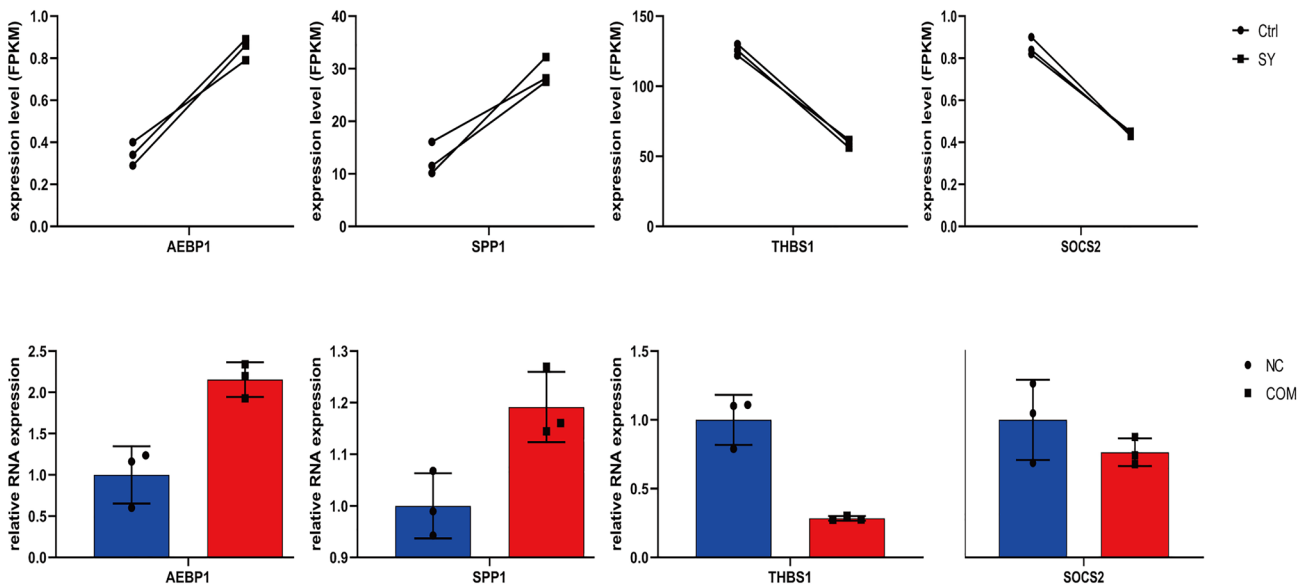
Fig. 3 Validation of the expression of important genes involved in nephrolithiasis. **A** Box plot showing the expression levels of differentially expressed genes (DEGs) involved in cell adhesion, extracellular matrix organization, extracellular matrix disassembly, inflammatory responses, and negative regulation of apoptosis, as indicated by term annotation analysis. **B** Scatter plot showing the results of RNA sequencing and RT-qPCR as the means ± standard deviations, with indicated statistically significant differences between groups ($p < 0.05$)

Furthermore, we established the regulatory network of TFs that undergo variable splicing and mediate DEG expression (Fig. 6). Additionally, we identified and demonstrated the involvement of important TFs in

the regulatory network (for instance, IRF3, STAT family members, TBP, ZNF143, and NR2F2) with DEGs in the regulatory processes of cell adhesion, inflammatory response, extracellular matrix composition, cell
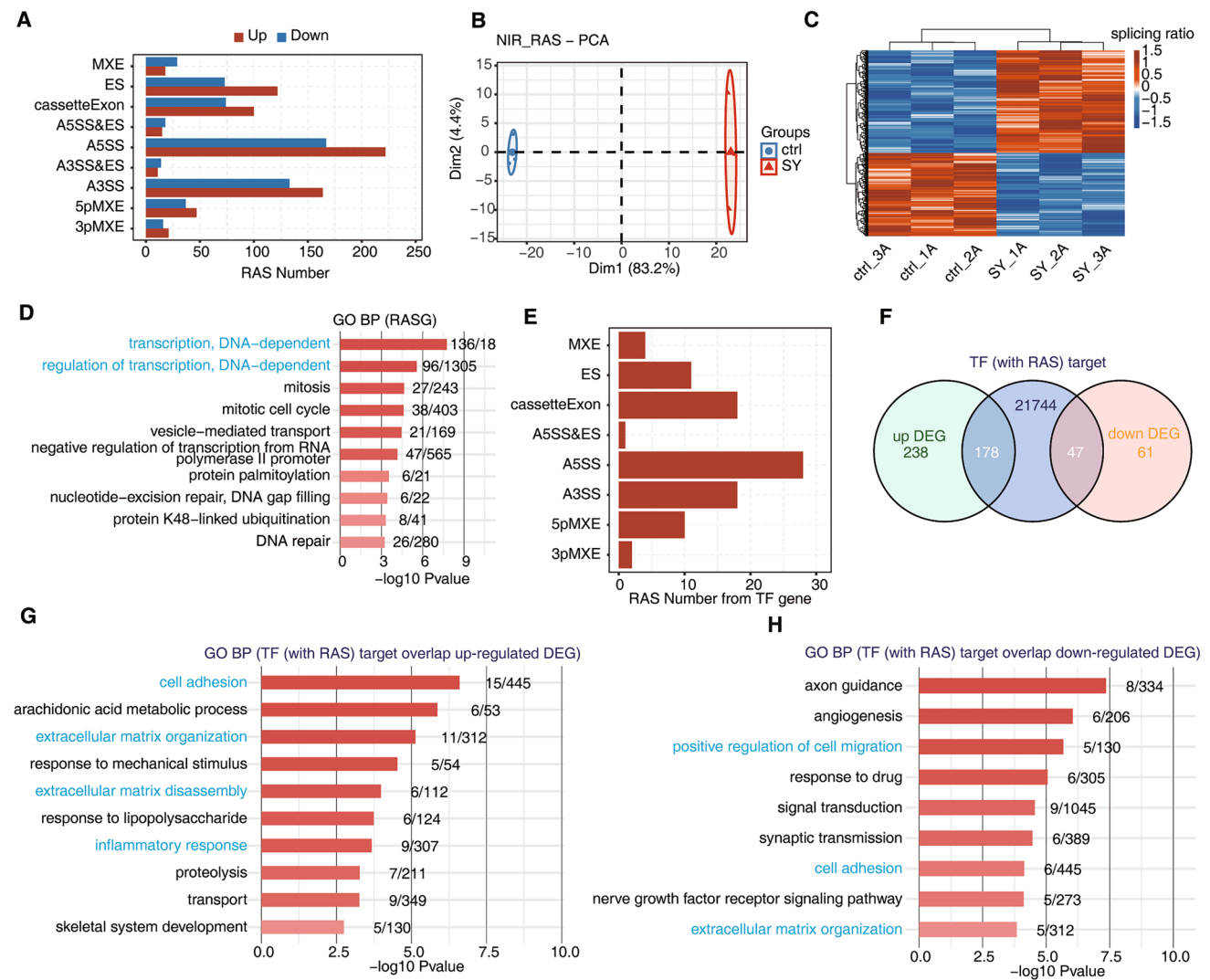
Fig. 4 Global features and enriched functions of deregulated alternative splicing events between treated and control samples. **A** Classification of all regulated alternative splicing events (RASEs). X-axis: Number of RASEs. **B** Principal component analysis (PCA) of SY and control (Ctrl) human renal tubular epithelial cells based on the percentage of spliced (PSI) values of all nonintron-retained (NIR) splice events. The ellipse for each group is the confidence ellipse. **C** PSI heat map of all NIR RASEs in SY samples compared to Ctrl samples. The filtration criteria used to identify an ASE were detectable splice junctions in all samples and at least 80% of the samples having 10 or more splice junction reads. **D** Gene ontology (GO) analysis of regulatory alternatively spliced genes (RASGs) in SY samples compared to Ctrl samples. **E** Classification of RASEs in transcription factors (TFs). *X*-axis: number of RASEs. **F** Venn diagram of TF targets with regulated alternative splicing and up- and downregulated genes. TF targets were identified using the Ensembl database and TRRUST database (https://www.grnpedia.org/trrust/). **G** Top 10 GO biological process terms most enriched by upregulated DEGs overlapping with TF (with RAS) target genes. **H** Top 10 GO biological process terms most enriched by downregulated DEGs overlapping with TF (with RAS) gene targets

migration, etc. Pathways involved in cell adhesion (CD22, SPP1, AEBP1, etc.) and the inflammatory response (GPR68, S100A9, FOS, etc.) were significantly upregulated, while those involved in cell migration-related genes (THBS1) were significantly downregulated, suggesting an altered functional state of the cells.

Discussion

ASEs exert important effects on the regulation of gene expression and contribute to the diversification of gene expression and protein properties. ASEs have also been a
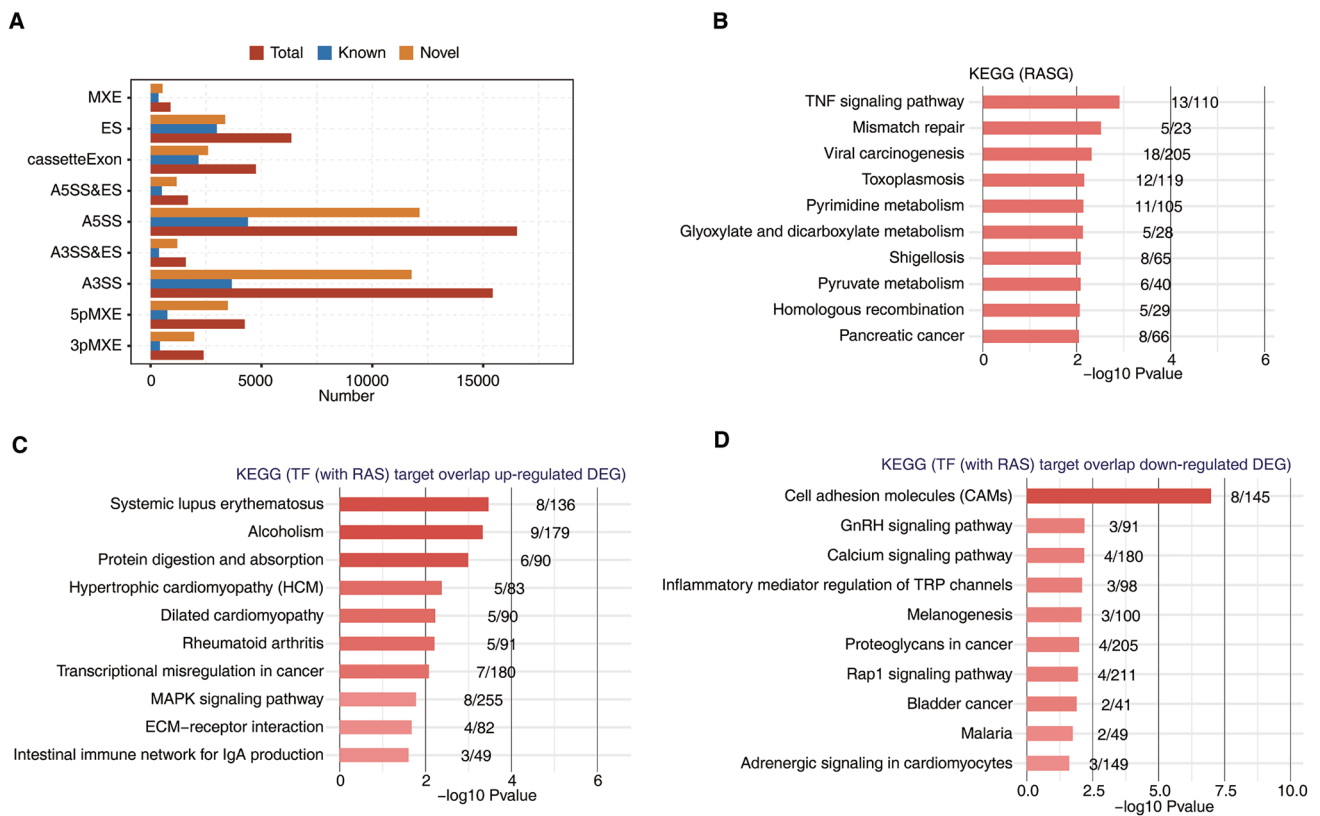
Fig. 5 Global features and enriched functional terms associated with dysregulated alternative splicing events (ASEs) between treated and control samples. **A** Bar plot showing the number of known and novel detected ASEs, which were classified into 9 types. **B** Kyoto Encyclopedia of Genes and Genomes (KEGG) analysis of regulatory alter-natively spliced genes (RASGs) in SY samples and control (Ctrl) samples. **C** Top 10 KEGG terms most enriched by upregulated DEGs overlapping with TF (with RAS) target genes. **D** Top 10 KEGG terms most enriched by downregulated DEGs overlapping with TF (with RAS) target genes
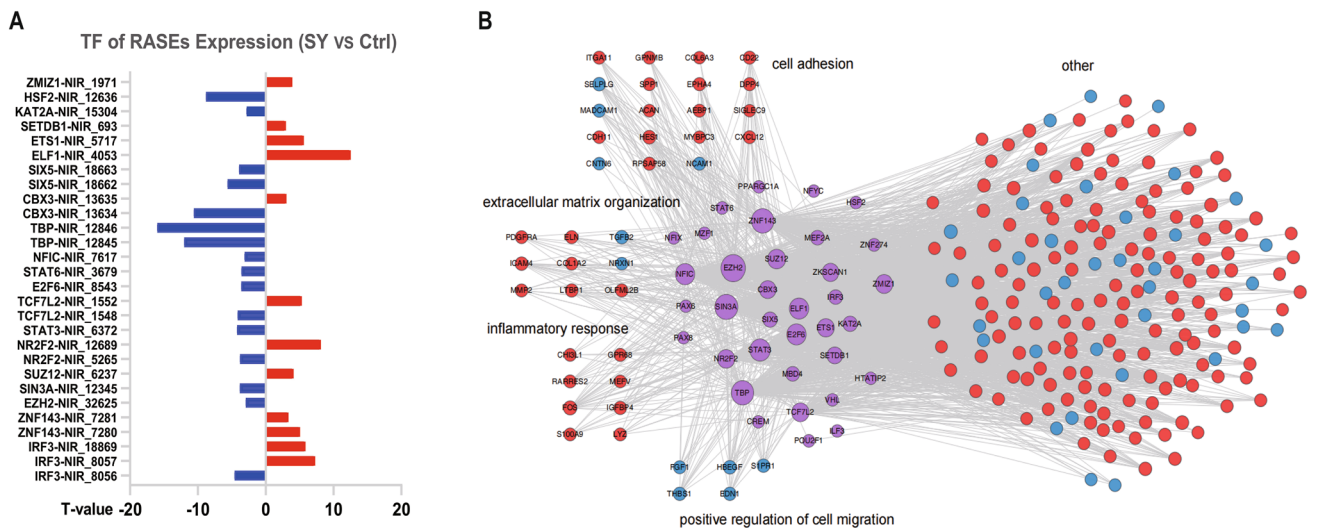
Fig. 6 Transcription factor–differentially expressed gene (TF–DEG) network comprising TFs (middle) and DEGs. **A** Differences in the expression of different spliceosomes of TFs with regulated alternative splicing. **B** TFs were significantly associated with cell adhesion, inflammatory responses, extracellular matrix organization, positive regulation of cell migration and other processes. Differences in spli-ceosomes are expressed as *T* values, and *P* < 0.05 was considered significant for the experimental group compared with the control group. Only TF–DEG connections found in the Ensemble or TTRUST database were included in the network. DEGs were classified according to Gene Ontology (GO) terms. Red circles indicate upregulated genes, and blue circles indicate downregulated genes

hot spot in the field of RNA-seq analysis and drug development [14, 15]. Studies on renal ASEs have been reported, for instance, by Jing et al., regarding the involvement of alternative splicing of circular RNAs (circRNAs) in the regulation of renal cancer specificity [16]. Wineberg et al. studied the regulatory role of mRNA AS at the single-cell level in kidney development and differentiation [17]. However, few ASEs have been reported in studies on urinary stones, which characterize a major kidney disease. Our study aimed to fill this gap.

In previous studies on the effects of crystal deposition on gene expression in renal tissue, Khan et al. used the ethylene glycol (EG) model and found that crystal retention may cause genetic alterations in inflammatory factors [18]. Koul et al. showed that HK-2 cells undergo compositional changes and altered biological processes when stimulated with different oxalates [19]. Recently, a data set from Randall's plaque also showed that CaOx causes pro-oxidative and pro-damage gene expression alterations [20]. We believe that the differences in our data are due to the different choices of mold-making methods. We innovatively used nanocrystals formulated from clinical stones to stimulate renal tubular epithelial cells and investigated the effects of this stimulation on genomic changes and selective splicing events. Interestingly, we found that crystal deposition can cause changes in renal tubular epithelial adhesion processes as well as inflammatory damage to renal tissue, which is consistent with the previous studies.

Based on RASE analysis and functional clustering analysis of associated genes, we established a network map showing the regulation of gene expression by ASEs and found that AS genes are highly concentrated in transcriptional regulatory pathways. In stone formation, ASEs in TFs can regulate cell adhesion, apoptosis (particularly affecting negative regulation), and tissue inflammatory responses. Crystallographic cell adhesion remains an important process in the development of renal calculi [2, 5, 21]. Crystallization stimulation may induce an immune response in renal tubular epithelial cells and affect changes in cellular functions [22]. Among these changes, oxidative damage has been reported most frequently. Increased intracellular generation of reactive oxygen species (ROS) can induce changes in gene expression and even lead to DNA damage [23]. Oxidative stress may be the cause of increased ASEs. The transcription factors identified herein, such as IRF3, STAT3, TBP, SIN3A, and PAX8, have been reported to be involved in transcriptional regulation [24–28]. For example, STAT3 and IRF3 can affect human immune processes and the cell cycle through transcriptional regulation [24, 29].

In injury caused by renal stone crystal deposition, we reported that AEBP1, SPP1, THBS1, ITGA11, and SOCS2 may be involved in transcriptional regulation. Based on previous studies, we determined that injury caused by crystal deposition is frequently accompanied by renal fibrosis and that THBS1, ITGA11, and SOCS2 can affect the fibrotic process [30–32]. Moreover, Murphy et al. found that THBS1 promoted tissue fibrosis by activation of the TGF-B pathway [33]. We were particularly intrigued by the study by Cao's team, which showed that THBS1 increased cell adhesion and migration via the YAK/FAK signaling pathway [34]. The downregulation of THBS1 expression was inferred as a possible protective factor against injury by renal stone crystal deposition, protecting the renal tubular epithelium from crystal damage, promoting fiber repair and reducing the cell adhesion capacity. However, further experiments are needed to confirm this inference. In contrast, Liu et al. found that AEBP1 activated the NF-kB pathway and affected the growth state of cells [35, 36]. In addition, Deng, Wang et al. found that SPP1 promoted cell proliferation and migration through the NF-kB pathway [37, 38]. Overall, all identified genes regulated by ASEs affect cell adhesion, damage repair, inflammatory signaling activation and other cellular activities associated with kidney stones.

In the TF–DEG regulatory network, CD22 was differentially expressed. CD22 is a cell-surface B cell-specific receptor involved in cell adhesion and signaling processes [39]. In the development of kidney stones, CD22 may be involved in recruiting leukocytes and triggering the inflammatory response [40]. This study is the first to describe CD22 involvement in kidney stone disease. Previously described adhesion molecules in renal stone disease include CD44, HA, and OPN [21, 41]. In our study, the involvement of CD22 might be related to leukocyte chemotaxis and in vivo clearance of crystals, which are possibilities that need to be further investigated.

In summary, our report of selective splicing events in kidney stone formation fills a gap in the field of AS in basic research on kidney stones. The analytical results provide new insights into the mechanism of urinary stone formation and provide a basis for subsequent research on the specific regulatory mechanism(s) of ASEs and kidney stone formation.

Declarations

Conflict of interest The authors declare that they do not have any conflicts of interest.

Ethical approval This article does not concern any author's involvement in human or animal studies.

References

1. Scales CD Jr, Tasian GE, Schwaderer AL, Goldfarb DS, Star RA, Kirkali Z (2016) Urinary stone disease: advancing knowledge, patient care, and population health. Clin J Am Soc Nephrol 11(7):1305–1312. https://doi.org/10.2215/CJN.13251215

2. Thongboonkerd V (2019) Proteomics of crystal-cell interactions: a model for kidney stone research. Cells 8(9):1076. https://doi.org/10.3390/cells8091076

3. Li L, Peng Y, Liu M et al (2019) Apoptosis of human kidney epithelial cells induced by high oxalate and calcium oxalate monohydrate is apurinic/apyrimidinic endonuclease 1 pathway dependent and contributes to kidney stone formation. Discov Med 28(152):75–85

4. Rao CY, Sun XY, Ouyang JM (2019) Effects of physical properties of nano-sized hydroxyapatite crystals on cellular toxicity in renal epithelial cells. Mater Sci Eng C Mater Biol Appl 103:109807. https://doi.org/10.1016/j.msec.2019.109807

5. Khamchun S, Thongboonkerd V (2018) Cell cycle shift from G0/G1 to S and G2/M phases is responsible for increased adhesion of calcium oxalate crystals on repairing renal tubular cells at injured site. Cell Death Discov 4:106. https://doi.org/10.1038/s41420-018-0123-9

6. Chen Y et al (2019) Harnessing calcium-oxalate- (CaOx-) nanocrystal-induced prodeath autophagy for attenuating human renal proximal tubular epithelial cell injury. Part Part Syst Charact 36(8):1900083

7. Kim D, Pertea G, Trapnell C, Pimentel H, Kelley R, Salzberg SL (2013) TopHat2: accurate alignment of transcriptomes in the presence of insertions, deletions and gene fusions. Genome Biol 14(4):R36. https://doi.org/10.1186/gb-2013-14-4-r36

8. Robinson MD, McCarthy DJ, Smyth GK (2010) edgeR: a bioconductor package for differential expression analysis of digital gene expression data. Bioinform (Oxf Engl) 26(1):139–140. https://doi.org/10.1093/bioinformatics/btp616

9. Xia H, Chen D et al (1860) (2017) CELF1 preferentially binds to exon-intron boundary and regulates alternative splicing in HeLa cells. Biochimica et Biophysica Acta. Gene Regul Mech 9:911–921. https://doi.org/10.1016/j.bbagrm.2017.07.004

10. Jin L, Li G, Yu D, Huang W, Cheng C, Liao S, Wu Q, Zhang Y (2017) Transcriptome analysis reveals the complexity of alternative splicing regulation in the fungus Verticillium dahliae. BMC Genom 18(1):130. https://doi.org/10.1186/s12864-017-3507-y

11. Xie C, Mao X, Huang J, Ding Y, Wu J, Dong S, Kong L, Gao G, Li CY, Wei L (2011) KOBAS 2.0: a web server for annotation and identification of enriched pathways and diseases. Nucl Acids Res 39((Web Server issue)):W316–W322. https://doi.org/10.1093/nar/gkr483

12. Slewinski TL, Anderson AA, Zhang C, Turgeon R (2012) Scarecrow plays a role in establishing Kranz anatomy in maize leaves.

13. Goeman JJ, van de Geer SA, de Kort F, van Houwelingen HC (2004) A global test for groups of genes: testing association with a clinical outcome. Bioinform (Oxf Engl) 20(1):93–99. https://doi.org/10.1093/bioinformatics/btg382

14. Saraiva-Agostinho N, Barbosa-Morais NL (2019) psichomics: graphical application for alternative splicing quantification and analysis. Nucl Acids Res 47(2):e7. https://doi.org/10.1093/nar/gky888

15. Zhao S (2019) Alternative splicing, RNA-seq and drug discovery. Drug Discov Today 24(6):1258–1267. https://doi.org/10.1016/j.drudis.2019.03.030

16. Feng J, Chen K, Dong X, Xu X, Jin Y, Zhang X, Chen W, Han Y, Shao L, Gao Y, He C (2019) Genome-wide identification of cancer-specific alternative splicing in circRNA. Mol Cancer 18(1):35. https://doi.org/10.1186/s12943-019-0996-0

17. Wineberg Y, Bar-Lev TH, Futorian A, Ben-Haim N, Armon L, Ickowicz D, Oriel S, Bucris E, Yehuda Y, Pode-Shakked N, Gilad S, Benjamin S, Hohenstein P, Dekel B, Urbach A, Kalisky T (2020) Single-cell RNA sequencing reveals mRNA splice isoform switching during kidney development. J Am Soc Nephrol 31(10):2278–2291. https://doi.org/10.1681/ASN.2019080770

18. Joshi S, Wang W, Khan SR (2017) Transcriptional study of hyperoxaluria and calcium oxalate nephrolithiasis in male rats: Inflammatory changes are mainly associated with crystal deposition. PLoS One 12(11):e0185009. https://doi.org/10.1371/journal.pone.0185009

19. Koul S, Khandrika L, Meacham RB, Koul HK (2012) Genome wide analysis of differentially expressed genes in HK-2 cells, a line of human kidney epithelial cells in response to oxalate. PLoS One 7(9):e43886. https://doi.org/10.1371/journal.pone.0043886

20. Taguchi K, Hamamoto S, Okada A, Unno R, Kamisawa H, Naiki T, Ando R, Mizuno K, Kawai N, Tozawa K, Kohri K, Yasui T (2017) Genome-wide gene expression profiling of randall's plaques in calcium oxalate stone formers. J Am Soc Nephrol 28(1):333–347. https://doi.org/10.1681/ASN.2015111271

21. Asselman M, Verhulst A, De Broe ME, Verkoelen CF (2003) Calcium oxalate crystal adherence to hyaluronan-, osteopontin-, and CD44-expressing injured/regenerating tubular epithelial cells in rat kidneys. J Am Soc Nephrol 14(12):3155–3166. https://doi.org/10.1097/01.asn.0000099380.18995.f7

22. Knauf F, Brewer JR, Flavell RA (2019) Immunity, microbiota and kidney disease. Nat Rev Nephrol 15(5):263–274. https://doi.org/10.1038/s41581-019-0118-7

23. Joshi S, Khan SR (2019) Opportunities for future therapeutic interventions for hyperoxaluria: targeting oxidative stress. Expert Opin Ther Targets 23(5):379–391. https://doi.org/10.1080/14728222.2019.1599359

24. Hillmer EJ, Zhang H, Li HS, Watowich SS (2016) STAT3 signaling in immunity. Cytokine Growth Factor Rev 31:1–15. https://doi.org/10.1016/j.cytogfr.2016.05.001

25. Ferraiuolo M, Di Agostino S, Blandino G (2016) Oncogenic Intra-p53 family member interactions in human cancers. Front Oncol 6:77. https://doi.org/10.3389/fonc.2016.00077

26. Li CG, Nyman JE, Braithwaite AW, Eccles MR (2011) PAX8 promotes tumor cell growth by transcriptionally regulating E2F1 and stabilizing RB protein. Oncogene 30(48):4824–4834. https://doi.org/10.1038/onc.2011.190

27. Erhard F, Baptista M, Krammer T, Hennig T, Lange M, Arampatzi P, Jürges CS, Theis FJ, Saliba AE, Dölken L (2019) scSLAM-seq reveals core features of transcription dynamics in single cells. Nature 571(7765):419–423. https://doi.org/10.1038/s41586-019-1369-y

28. Lu W, Chen Z, Zhang H, Wang Y, Luo Y, Huang P (2012) ZNF143 transcription factor mediates cell survival through upregulation of

the GPX1 activity in the mitochondrial respiratory dysfunction. Cell Death Dis 3(11):e422. https://doi.org/10.1038/cddis.2012. 156

29. Jefferies CA (2019) Regulating IRFs in IFN driven disease. Front Immunol 10:325. https://doi.org/10.3389/fimmu.2019.00325

30. Ye J, Lin Y, Yu Y, Sun D (2020) LncRNA NEAT1/microRNA-129-5p/SOCS2 axis regulates liver fibrosis in alcoholic steatohepatitis. J Transl Med 18(1):445. https://doi.org/10.1186/s12967-020-02577-5

31. Jiang D, Guo B, Lin F, Lin S, Tao K (2020) miR-205 inhibits the development of hypertrophic scars by targeting THBS1. Aging 12(21):22046–22058. https://doi.org/10.18632/aging.104044

32. Bansal R, Nakagawa S, Yazdani S, van Baarlen J, Venkatesh A, Koh AP, Song WM, Goossens N, Watanabe H, Beasley MB, Powell CA, Storm G, Kaminski N, van Goor H, Friedman SL, Hoshida Y, Prakash J (2017) Integrin alpha 11 in the regulation of the myofibroblast phenotype: implications for fibrotic diseases. Exp Mol Med 49(11):e396. https://doi.org/10.1038/emm.2017.213

33. Murphy-Ullrich JE, Suto MJ (2018) Thrombospondin-1 regulation of latent TGF-β activation: a therapeutic target for fibrotic disease. Matrix Biol J Int Soc Matrix Biol 68–69:28–43. https://doi.org/10.1016/j.matbio.2017.12.009

34. Shen J, Cao B, Wang Y, Ma C, Zeng Z, Liu L, Li X, Tao D, Gong J, Xie D (2018) Hippo component YAP promotes focal adhesion and tumour aggressiveness via transcriptionally activating THBS1/FAK signalling in breast cancer. J Exp Clin Cancer Res CR 37(1):175. https://doi.org/10.1186/s13046-018-0850-z

35. Liu JY, Jiang L, Liu JJ et al (2018) AEBP1 promotes epithelial-mesenchymal transition of gastric cancer cells by activating the NF-κB pathway and predicts poor outcome of the patients. Sci Rep 8(1):11955. https://doi.org/10.1038/s41598-018-29878-6

36. Sinha S, Renganathan A, Nagendra PB, Bhat V, Mathew BS, Rao M (2019) AEBP1 down regulation induced cell death pathway depends on PTEN status of glioma cells. Sci Rep 9(1):14577. https://doi.org/10.1038/s41598-019-51068-1

37. Deng G, Zeng F, Su J, Zhao S, Hu R, Zhu W, Hu S, Chen X, Yin M (2020) BET inhibitor suppresses melanoma progression via the noncanonical NF-κB/SPP1 pathway. Theranostics 10(25):11428–11443. https://doi.org/10.7150/thno.47432

38. Wang Y, Su J, Wang Y, Fu D, Ideozu JE, Geng H, Cui Q, Wang C, Chen R, Yu Y, Niu Y, Yue D (2019) The interaction of YBX1 with G3BP1 promotes renal cell carcinoma cell metastasis via YBX1/G3BP1-SPP1- NF-κB signaling axis. J Exp Clin Cancer Res CR 38(1):386. https://doi.org/10.1186/s13046-019-1347-0

39. Sieger N, Fleischer SJ, Mei HE, Reiter K, Shock A, Burmester GR, Daridon C, Dörner T (2013) CD22 ligation inhibits downstream B cell receptor signaling and Ca(2+) flux upon activation. Arthritis Rheum 65(3):770–779. https://doi.org/10.1002/art.37818

40. Habtezion A, Nguyen LP et al (2016) Leukocyte trafficking to the small intestine and colon. Gastroenterology 150(2):340–354. https://doi.org/10.1053/j.gastro.2015.10.046

41. Qi S, Wang Q, Xie B, Chen Y, Zhang Z, Xu Y (2020) P38 MAPK signaling pathway mediates COM crystal-induced crystal adhesion change in rat renal tubular epithelial cells. Urolithiasis 48(1):9–18. https://doi.org/10.1007/s00240-019-01143-z

Publisher's Note Springer Nature remains neutral with regard to jurisdictional claims in published maps and institutional affiliations.